Polymer Chemistry

Synthesis and Characterization of Imidazolium-Mediated Tröger's Base Containing Poly(amide)-Ionenes and Composites with Ionic Liquids for CO2 Separation Membranes

Journal:	*Polymer Chemistry*
Manuscript ID	PY-ART-07-2020-001038.R1
Article Type:	Paper
Date Submitted by the Author:	20-Oct-2020
Complete List of Authors:	Kammakakam, Irshad; The University of Alabama, Chemical & Biological Engineering Bara, Jason; The University of Alabama, Chemical & Biological Engineering Jackson, Enrique; NASA Marshall Space Flight Center

Synthesis and Characterization of Imidazolium-Mediated Tröger's Base Containing Poly(amide)-Ionenes and Composites with Ionic Liquids for CO_2 Separation Membranes

Irshad Kammakakam,[†] Jason E. Bara,[†*] and Enrique M. Jackson[‡]

[†] *University of Alabama, Department of Chemical & Biological Engineering, Tuscaloosa, AL 35487-0203 USA*
[‡] *NASA Marshall Space Flight Center, Huntsville, AL 35812*

[*]Corresponding author. e-mail: jbara@eng.ua.edu

ABSTRACT

Considerable attention has been given to polymeric membranes either containing, or built from, ionic liquids (ILs) in gas separation processes due to their selective separation of CO_2 molecules. Achieving high-performance CO_2 separation membranes with enhanced permeability and selectivity relies mainly on rationally designing of the molecular substructure and molecular composition of the polymer matrix. In this work, we have exclusively explored a facile synthetic route to incorporate aromatic amide linkages onto ionene backbone derived from imidazolium-mediated Tröger's base moieties, yielding a novel rigid polyamide-ionene material ("Im-TB-PA ionene"). We have optimized two novel Im-TB-PA ionene polymers via Menshutkin reactions between *N,N′*-(1,4-phenylene)bis(4-(chloromethyl)benzamide) and equimolar amounts of two isomeric diimidazole-functionalized Tröger's base monomers with '*ortho'* or '*para'* regiochemistry. The two resulting Im-TB(*o*&*p*)-PA ionenes exhibited high molecular weights and excellent solubilities in polar organic solvents, serving homogeneous and mechanically stable blend membranes with "free" ILs. The structural and physical properties, as well as the gas separation behaviors of both the Im-TB(*o*&*p*)-PA ionenes and their IL composite counterparts ([Im-TB(*o*&*p*)-PA]+[IL]) were further extensively investigated. The membrane with an optimal composition and polymer architecture ([Im-TB(*o*)-PA]+[IL]) exhibited outstanding permselectivites for CO_2/CH_4 (46.73), CO_2/N_2 (51.74), and CO_2/H_2 (4.38) gas pairs together with the best CO_2 permeability of 47.2 barrer. Overall, this study provides a promising strategy to explore the benefits of Im-TB-PA ionenes to separate CO_2 from flue gas, natural gas, and syngas streams, while opening new possibilities in polymer design with strong candidate materials for other practical applications.

1. INTRODUCTION

Energy-efficient separation of acid gases such as CO_2, H_2S, and other organosulfur components is a challenging task of environmental significance as well as industrial application. Specifically, the removal of CO_2 has always been an important part of separation processes because of its high abundance and extremely low heating value in gas mixtures.[1-3] Over the past few decades, the development of polymeric membranes for effective CO_2 removal from gas mixtures at various pressures and compositions such as CO_2/N_2 (i.e., flue gas streams),[4, 5] CO_2/CH_4 (i.e., natural gas or biogas streams)[6, 7] and CO_2/H_2 (i.e., fuel gas or syngas)[8] has emerged as an active area of research in separation processes. It is always desirable to expand the spectrum of high-performance polymers to compete with well-established conventional separation processes including absorption,[9, 10] pressure swing adsorption (PSA),[11, 12] and cryogenic distillation[13] as polymeric membranes suffer a trade-off relationship between permeability (P) and selectivity (α), defining as so-called "upper bound" on the separation efficiency for each gas pair.[14, 15]

An ever-growing library of scientific literature reports on the selective CO_2 separation performance of membranes containing many different polymer families including polycarbonates,[16, 17] poly (phenylene oxide),[18] polyacetylenes,[19] polyaniline,[20] polypyrrolones,[21] poly (ethylene oxides),[22] polyketones,[23] polysulfones,[24] polyamides,[25, 26] and polyimides.[27, 28] A fundamentally different approach to the preparation of highly CO_2 permeable polymeric materials with ladder backbone structures and high fractional free volume (FFV) were reported by Budd and McKeown.[29] This novel microporous networked 'polymers of intrinsic microporosity' (PIMs) have expanded enormously and they are now promising candidates for the enhanced gas separation applications, especially for CO_2/light gas separations.[30-34] A recent effective integration of this

ladder-type microporous polymers is the incorporation of a kinked V-shaped tertiary amine diazocine bridged unit, which is more commonly known as Tröger's base (TB). The V-shaped cavities within TB units have introduced into PIMs either by TB forming polymerization reactions[35-37] or by polycondensation reaction of TB-containing monomers,[38-40] and yielding high-performance CO_2/light gas separation membranes which outperform the "upper bound" curves.

On the other hand, from a materials standpoint, the combination of ionic liquids (ILs) with polymeric membranes has widely been accepted as a promising approach to new CO_2 separation materials due to their high CO_2 solubility, and hence, high CO_2 gas selectivities over other common gases (N_2 and CH_4). Including our previous works, a wide variety of polymeric membranes either containing or built from ILs have been the increasing interest in membrane separation technology for enhanced CO_2 separation over the past two decades.[41-48] Among them, membranes prepared from polymeric ILs, also known as poly(IL)s, represent the most primitive and active approach for the design of CO_2 separation membranes employing moderate gas separation properties together with superior mechanical properties.

Our recent works on IL-inspired platforms are driven by ionenes wherein imidazolium cations were introduced as the backbone constitutes for high-performance CO_2 separation polymeric materials. A handful of examples have examined the novel synthetic steps and structure-property relationships as well as gas permeation behaviors of ionenes containing alternative functionalities typically seen in other high-performance polymers such as polyimide (PI) and polyamide (PA).[49-52] In a very recent study, we considered the benefits of above-mentioned TB-based polymers and ILs to produce a novel imidazolium-mediated Tröger's base-containing ionene polymer ("Im-TB-

Ionenes"), and extensively investigated the potential use of corresponding membranes for enhanced CO_2 separation.[53]

In our recent studies of "Im-TB-Ionene" gas separation membranes, we found that the molecular substructure of Im-TB units is highly amenable to incorporate into polymer chains, subscribing a variety of polymer structures not limited to just gas separations[38, 54] but many other applications such as CO_2 capture,[55, 56] catalysis,[57] and electrochemical applications.[58, 59] Therefore, considering our quest for the new development in "Im-TB-Ionenes", in this work we explore a full synthetic route to incorporate aromatic amide linkages onto ionene backbone neighboring with imidazolium-TB moieties, yielding a novel rigid polyamide ionene material ("Im-TB-PA"). As depicted in Chart 1, we optimized the molecular architecture for preparing durable Im-TB-PA ionene polymers with *N,N′*-(*p*-phenylene)dibenzamide linkages as the key structural moieties via Menshutkin reactions between *N,N′*-(1,4-phenylene)bis(4-(chloromethyl)benzamide) and an equivalent amount of TB-based-imidazole precursors (either *ortho* or *para* connectivity, Im-TB(*o*) or Im-TB(*p*)) and examined the structure-property relationships as well as gas transport properties of corresponding membranes. We also investigated the viability of newly developed "Im-TB-PA" ionenes to form high-stability composite membranes composed of "free" IL ($[C_4mim][Tf_2N]$), which imparted a high affinity toward CO_2 gas separation.

Chart 1. Structures of new ionenes: (a) Im-TB(*o*)-PA and (b) Im-TB(*p*)-PA developed in this study.

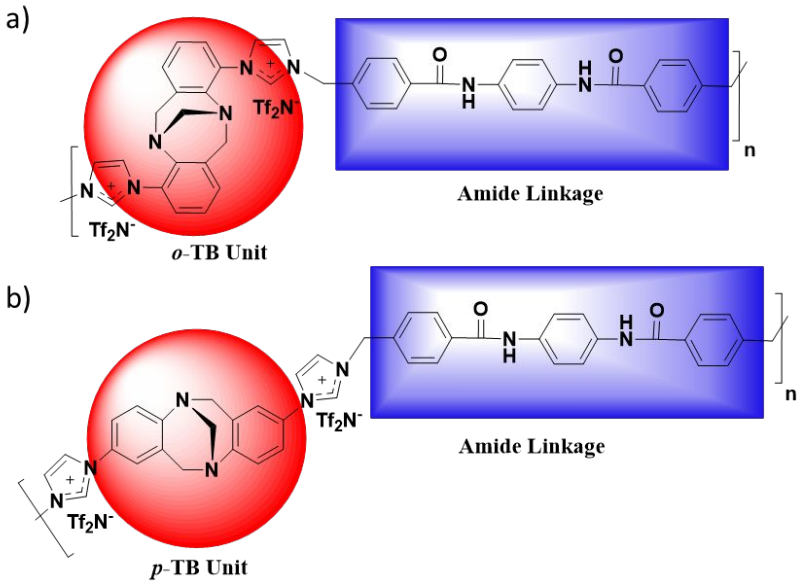

2. EXPERIMENTAL SECTION

2.1. Materials. 2-fluoronitrobenzene, 4-fluoronitrobenzene, and trifluoroacetic acid were purchased from Oakwood Chemical. Imidazole (99%) was purchased from Aldrich. Potassium carbonate (99%, anhydrous) and Pd/C (10% on C, Type 487) were purchased from BeanTown Chemical. Paraformaldehyde (>97%) was obtained from Alfa Aesar. 4-(chloromethyl) benzoyl chloride and α, α'-Dichloro-p-xylene (>98%) was purchased from TCI. Lithium bis-trifluoromethanesulfonimide (HQ-115) was purchased from 3M. Ethanol (200 proof), N-methylpyrrolidone (NMP) (ACS grade), and Dimethylacetamide (DMAc) (ACS grade) were purchased from VWR. Celite 545 was purchased from Acros Organics.

The "free" IL [C_4mim][Tf_2N] was prepared from 1-methylimidazole (99%, Aldrich) (St. Louis, MO, USA), 1-bromobutane (99%, Aldrich) (St. Louis, MO, USA), and LiTf_2N (99%, 3M) (Minneapolis, MN, USA) according to our previously reported procedure.[50, 60] The purity and

structure of [C_4mim][Tf_2N] were confirmed by ^{1}H NMR spectra (see Supporting Information Figure S1). All other chemicals were obtained from commercial sources and used as received.

2.2. Characterization. ^{1}H NMR spectra were acquired on a Bruker Avance (500 MHz) instrument using d6-DMSO as a reference or internal deuterium lock. FT-IR spectra of the materials were recorded using a Perkin-Elmer Spectrum 2 in the range of 4000–400 cm^{-1}. Molar masses were determined by matrix-assisted laser desorption/ionization time-of-flight mass spectrometry (MALDI-TOF MS, a Bruker Ultraflex instrument). Thermogravimetric analysis (TGA) of the polymer materials was conducted using Seiko TG-DTA 7300 by heating samples from r.t. to 700°C at a heating rate of 10°C/min under N_2 flow. The glass transition temperature (T_g) of each polymer material was measured using a DSC (TA Instruments, DSC Q20) from 20°C to 300°C with a scan rate of 10°C min-1 under N_2. The Wide-angle X-ray diffraction (WAXD) patterns of the membranes were measured using a Bruker D8 Discover diffractometer by employing a scanning rate of 4°/min in a 2θ range from 5° to 60° with a Co Kα1 X-ray (λ = 0.17886). The d-spacings values were calculated according to Bragg's law (d = λ/2 sinθ).

2.3. Synthesis of Imidazolium-Mediated TB Containing Polyamide Ionene Polymers (Im-TB-PA ionenes)

2.3.1. Synthesis of Tröger's Base-Containing Imidazole Monomers (Im-TBs). Both *ortho* and *para* isomers of Imidazole-TB monomers were prepared according to our previously reported procedure.[53] The purity and structures of these molecules were again confirmed by ^{1}H NMR analysis.

2.3.2. Synthesis of *N,N′*-(1,4-phenylene)bis(4-(chloromethyl)benzamide) (Amide Linkage). Following a literature method for the preparation of amide linkage,[61] into a 1000 mL round-bottom-flask equipped with a magnetic stir bar, a suspension of *p*-phenylenediamine (5 g, 46.23 mmol) in anhydrous CH_2Cl_2 (150 mL) was prepared and Et_3N (9.36 g, 92.47 mmol) was added dropwise. To this, a solution of 4-(chloromethyl) benzoyl chloride (17.48 g, 92.47 mmol) in anhydrous CH_2Cl_2 (250 mL) was added with vigorous stirring and continued for 18 h at room temperature. Then, the resultant mixture was filtrated off and washed with CH_2Cl_2 (3 × 100 mL) to obtain amide linkage product as colorless solid. Yield: 16.9 g (88%); ^{1}H NMR (500 MHz,DMSO-*d*6): δ 10.38 (s, 2H, 2×Ar–N*H*–C=O), 7.96 (d, 4H, Ar*H*), 7.74 (s, 4H, Ar*H*), 7.58 (d, 4H, Ar*H*), and 4.85 (s, 4H, 2×Ar–CH_2–Cl).

2.3.3. Synthesis of Two Novel Im-TB-PA Ionenes. Into a 250 mL heavy-walled round-bottom-flask (Ace Glass) equipped with a magnetic stir bar, Im-TB (either *ortho* or *para*, 4 g, 11.29 mmol) was dissolved with NMP (100 mL) and the corresponding equimolar amount of amide comonomer (4.66 mmol, 11.29 g) was added. Then, the flask was sealed with a threaded PTFE cap and DuPont Kalrez® o-ring, and the reaction mixture stirred at 110 °C until mixing became impossible due to polymer precipitation (~24 h). Afterward, the precipitated polymer product was cooled to r.t. and the remaining NMP was decanted, and deionized H_2O was added directly to the flask. The vessel was further heated to 40°C with vigorous stirring in order to dissolve the polymer solids in water. Meantime, $LiTf_2N$ (8.1 g, 28.2 mmol) was dissolved in 200 mL of DI water in a 500 mL Erlenmeyer flask, and the completely dissolved polymer product from the flask was poured into the aq. $LiTf_2N$ solution, whereupon a precipitate immediately formed. The mixture was vigorously stirred with an overhead mechanical stirrer for 1 h and the polymer was collected

by filtration and dried in a vacuum oven at 80 °C for 36 h to give desired Im-TB-PA ionene polymers.

Im-TB(*o*)-PA. Yield 12.2 g (86%); ^{1}H NMR (500 MHz, DMSO-d_6) δ 10.33 (s, 2H, 2×Ar–N*H*–C=O), 9.91 (s, 2H, 2×N=C*H*–N), 8.24 (s, 2H, 2×N–C*H*=C), 8.15-7.96 (br, 2H, 2×N–C*H*=C and 4H, Ar*H*), 7.87-7.57 (br, 4H, NH–Ar*H*–NH) 7.55-7.07 (br signal, 10H, Ar*H*), 5.88-5.50 (s, 4H, 2×Ar–CH_2–N) 4.56-4.18 (br signal, 4H, 2×Ar–CH_2–N and 2×N–C*H*–N) and 3.76-3.53 (br signal, 2H, 2×N–CH_2–Ar); (FT-IR)/cm^{-1} 3080, 1695, 1480, 1320, 1195, 1050, 750 and 640.

Im-TB(*p*)-PA. Yield 11.5 g (81%); ^{1}H NMR (500 MHz, DMSO-d_6) δ 10.34 (s, 2H, 2×Ar–N*H*–C=O), 9.93 (s, 2H, 2×N=C*H*–N), 8.25 (s, 2H, 2×N–C*H*=C), 8.17-7.99 (br, 2H, 2×N–C*H*=C and 4H, Ar*H*), 7.83-7.60 (br, 4H, NH–Ar*H*–NH) 7.58-7.10 (br signal, 10H, Ar*H*), 5.79-5.53 (s, 4H, 2×Ar–CH_2–N) 4.51-4.22 (br signal, 4H, 2×Ar–CH_2–N and 2×N–C*H*–N) and 3.70-3.54 (br signal, 2H, 2×N–CH_2–Ar); (FT-IR)/cm^{-1} 3082, 1695, 1480, 1320, 1195, 1050, 750 and 640.

2.4. Membrane Preparation. All the neat Im-TB-PA ionenes and corresponding "free" IL composite membranes were prepared by the solution casting method using DMAc (90wt %) as a solvent. Two molar equivalent amounts of "free" IL ([C_4mim] [Tf_2N], 0.667 g, 1.59 mmol) per polymer repeat unit were added into each Im-TB-PA ionene (1 g, 0.795 mmol) solution in order to obtain composite membranes ([Im-TB(o&p)-PA][IL]). All of the dope solutions were sonicated at 30°C until they form completely homogeneous. The resultant solutions were filtered through a cotton plug to ensure that the dope solutions were free of any dust particles and poured onto Teflon molds having 60 mm diameter well. The Teflon plates were then placed in an oven, covered with aluminum foils having small holes, and allowed to slow solvent evaporation at 40°C for 24 h. The oven temperature was slowly raised to 60 °C, 80 °C, and then 100 °C over the course of 48 h and

vacuumed for further 12h in order to remove the complete solvent. After becoming completely dried, the membranes were peeled off from the Teflon plate, and then being stored at the ambient temperature for later use. The thickness of the membranes was controlled to be 100 to 130 μm.

2.5. Gas Separation Measurements. The pure gas permeation measurements were performed to determine the gas separation properties of the newly developed Im-TB-PA ionenes and their IL composite counterpart membranes using a high-vacuum time lag apparatus according to the constant-volume/variable-pressure method, as described in our previous works[49, 53, 62] All permeation measurements were conducted at 20 °C and the feed pressure was ~3 atm (~45 psia) against initial downstream vacuum (<0.01 psia). Pressures and temperatures were monitored and recorded using most recent version of LabVIEW software (National Instruments). Both the feed and the permeate sides were thoroughly evacuated to remove any residual gases before each permeation measurement. The pressure rises versus time transient of the permeate side was recorded and passed to a desktop computer through a shield data cable. The permeability coefficient of each membrane was determined from the linear slope of the downstream pressure rise versus time plot (dp/dt) based on Equation 1:

$$P = \frac{273}{76} \times \frac{Vl}{AT\widetilde{p}} \times \frac{dp}{dt} \qquad (1)$$

where P is the permeability expressed in Barrer (1 barrer = 10^{-10} cm^3(STP)cm cm^{-2} s^{-1} cmHg^{-1}); V (cm^3) is the downstream volume; l (cm) is the thickness of the membrane; A (cm^2) is the effective gas permeation area of the membrane; T (K) is the measurement temperature; p_0 (in Torr) is the pressure of the feed gas at the upstream and dp/dt is the rate of the pressure rise under the steady state. The ideal permselectivity $(\alpha_{A/B})$ of each membrane for a pair of gases (A and B) was calculated from the ratio of the individual gas permeability coefficients as, P_A/P_B.

The diffusivity and solubility were obtained from the intercept according to Equations 2 and 3:

$$D = \frac{l^2}{6\theta} \qquad (2)$$

$$S = \frac{P}{D} \qquad (3)$$

where D ($cm^2.s^{-1}$) is the diffusivity coefficient, l is the membrane thickness (cm) and θ is the time lag (s), obtained from the intercept of the linear steady-state part of downstream pressure rise versus time plot. Solubility, S, was calculated from Eqn. (3) with respect to permeability and diffusivity obtained from Eqn. (1) and (2).

3. RESULTS AND DISCUSSION

3.1. Synthesis and Structural Characterization of Imidazolium-TB Containing Poly(amide) Ionene Polymers (Im-TB-PA Ionenes). As summarized in Scheme 1, two new Im-TB-PA ionene polymers were synthesized from the two-step reactions. Firstly, the amidation reaction of 4-(chloromethyl)benzoyl chloride and *p*-phenylenediamine was performed in the presence of triethylamine in CH_2Cl_2 to give the amide linkage monomer *N,N′*-(1,4-phenylene)bis(4-(chloromethyl)benzamide) as a white precipitate. The purity and structure of the amide linkage monomer were confirmed by ^{1}H NMR analysis (Figure S2). This amide linkage having an electrophilic benzyl chloride group at both termini was used as a dielectrophilic monomer in the second step of polymerization with equimolar amounts of two different Im-TB co-monomers (either '*ortho*' and '*para*') as dinucleophilic monomers via Menshutkin reactions to obtain two novel Im-TB-PA ionene polymers followed by an anion exchange reaction from halides to Tf_2N^- anions. The structural characterization of these newly developed Im-TB-PA ionenes was qualitatively analyzed by ^{1}H NMR (Figure 1) and FT-IR measurements (Figure S3). The ^{1}H NMR

spectra of the Im-TB-PA ionene polymers displayed the characteristic peaks of imidazolium protons at 9.93 ppm and bicyclic ring of Tröger's base protons in the region of 4.5–3.5 ppm, revealing the successful incorporation of imidazolium-TB groups in the ionene backbone. In addition, amine protons at 10.34 ppm and other protons at aromatic region of both Im-TB-PAs were further confirmed the presence of amide linkage in the respective ionene backbones, confirming the diverse structures of newly developed Im-TB-PA ionene polymers (Figure 1).

Scheme 1. Schematic representation of the preparation of new Im-TB-PA ionene polymers.

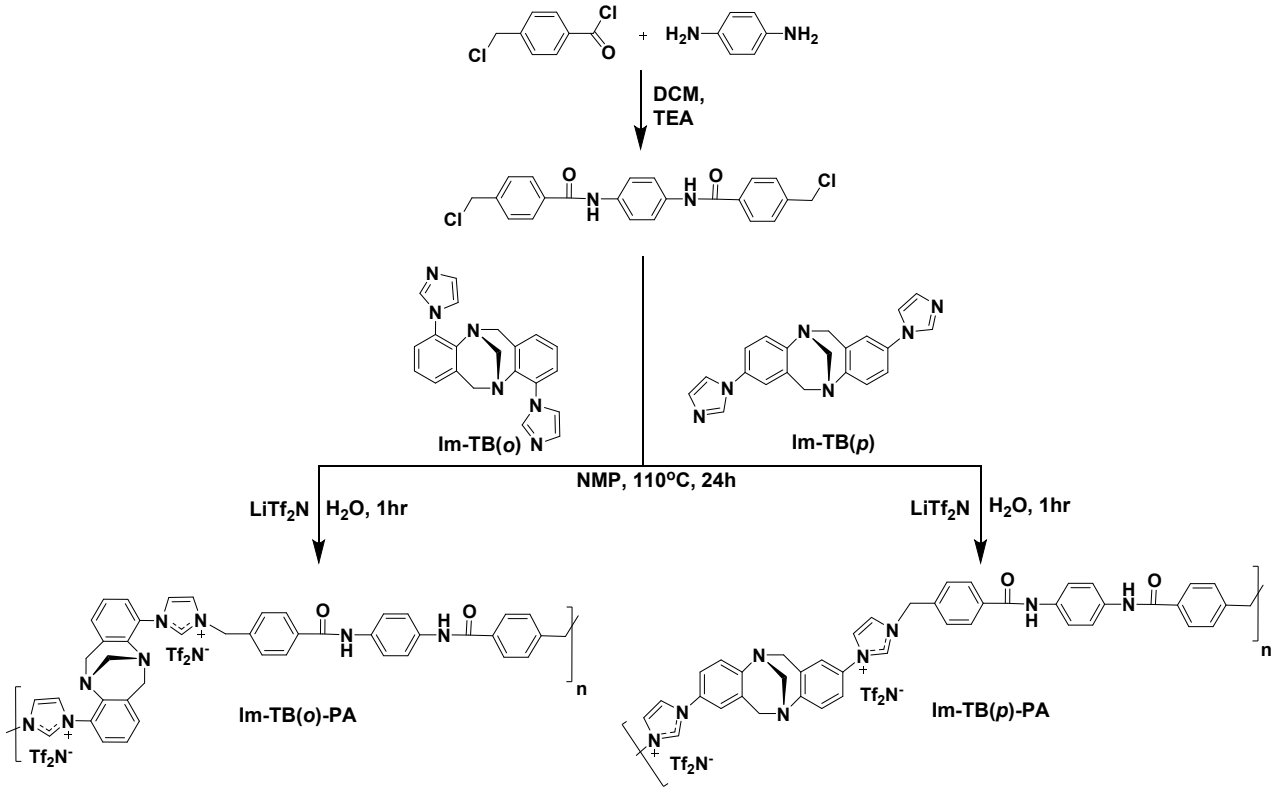

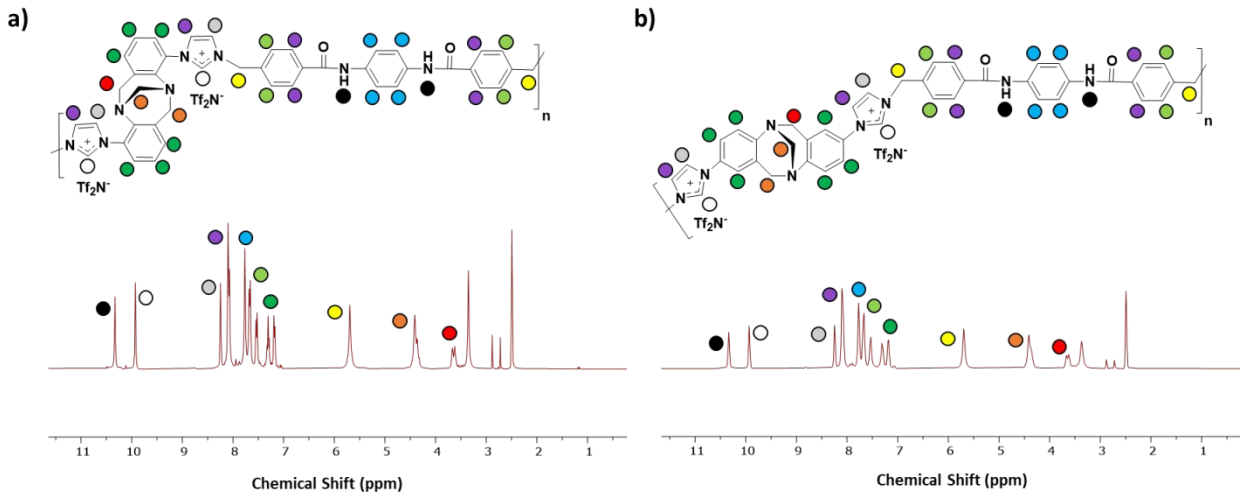

Figure 1. ^{1}H NMR spectra of (a) Im-TB(*o*)-PA and (b) Im-TB(*p*)-PA ionene polymers.

As seen in Figure S3, the FT-IR spectra also verified the chemical structures of Im-TB-PA ionene polymers. Both the Im-TB-PAs showed the characteristic peaks corresponding of aromatic Tröger's base groups (C-H, C-N and C=C stretching vibrations at 3080 cm^{-1}, 1695 $cm^{-1,}$ and 1480 cm^{-1}, respectively) as well as the ionic moieties such as imidazolium cations (C-N vibrations at 1320 cm^{-1}) and Tf_2N^- anions (SO_2 and S-N-S stretching vibrations at 1195 cm^{-1} and 1050 cm^{-1}, respectively), proving the successful formation of imidazolium-based TB ionene polymers having Tf_2N^- counter anions.[63, 64]

Nevertheless, it was very difficult to perform the quantitative analysis of the newly developed ionenes using a size exclusion chromatography (SEC) measurement due to the incompatibilities of ionenes with the column, a similar limitation also observed in our previous works.[49, 65] Therefore, both Im-TB-PA species were characterized using MALDI-TOF MS to determine its molecular weight (m/z). The MALDI-TOF MS data were collected by spotting DMAc solutions of each sample, topped with a trihydroxy-acetophenone or trans-2-[3-(4-tert-butylphenyl)-2-methyl-2-propenylidene] malononitrile matrix in MeOH. Both the Im-TB-PA ionenes were found

to have very high molecular weights ($M_{N,}$ m/z = 113352.91 for Im-TB(*o*)-PA and 80202.583 for Im-TB(*p*)-PA, Figures S5, 6). Interestingly, 'ortho' derived Im-TB(*o*)-PA displayed a noticeably higher molecular weight compared to the other isomer of 'para' Im-TB(*p*)-PA ionene, plausibly because of higher reactivity of Im-TB(o) isomer monomer as reported in our previous work.[53] The MALDI-TOF measured M_N values together with the repeating unit molecular weights and calculated number-average repeat units (X_N) are summarized in ESI (Table S1).

3.2. Membrane Fabrication and Shape Memory Properties. Both the newly developed Im-TB-PA ionenes demonstrated excellent solubility in common membrane casting solvents such as DMF, DMAc, DMSO, and NMP (Table S2), indicating the high prospect of the thin film-forming ability which are generally the basic requirements for the gas separation tests. Capable of being compacted, solid highly flexible free-standing membranes were formed by casting a DMAc solution of respective Im-TB-PA ionene polymers and their composites, followed by vacuum drying process (the optical images are shown in Figure 2). While both the neat Im-TB-PA ionene obtained robust transparent membranes, their composite analogies found to have semi-transparent or translucent membranes. This behavior was attributed plausibly due to the complex combination of many polar groups such as amide linkage, imidazolium ionenes, and "free" ILs in the composite matrix, and hence, forming various intermolecular interactions (e.g., ionic, H-bonding, π-π, and π-cation stacking). Similar behavior of strong molecular interactions between polymer chains was also reported for other polyamides having polar PEO units.[66]

Furthermore, the newly developed Im-TB-PA ionene membranes exhibited excellent shape-memory (SM) properties at elevated temperature (60 ^{O}C), particularly in the Im-TB(*o*)-PA ionene

membrane. Polymers possessing SM or elastomeric properties at elevated temperature have been demenostrated in diverse applications, and are currently of significant interest in 3D-printing applications. Design and developing of ionic polymers with elastomeric properties in 3D-printing technology have been exstensively reported by Long and his co-workers.[67, 68] Recently, we also have reported the unique SM property of the amide-based ionenes showing a rapid recovery of shape upon a heat process.[51] As depicted in Figure 2, a similar experiment was examined in this study, indicating more contemporary applications of the newly developed Im-TB-PA ionenes beyond gas separation arena. The Im-TB(*o*)-PA ionene film was wrapped around a glass rod at 60 ^{O}C to form a helix-shaped ribbon and allowed to cool to room temperature, and the glass rod was removed. The resultant curved film was recovered its flat shape when heated again to 60 ^{O}C.

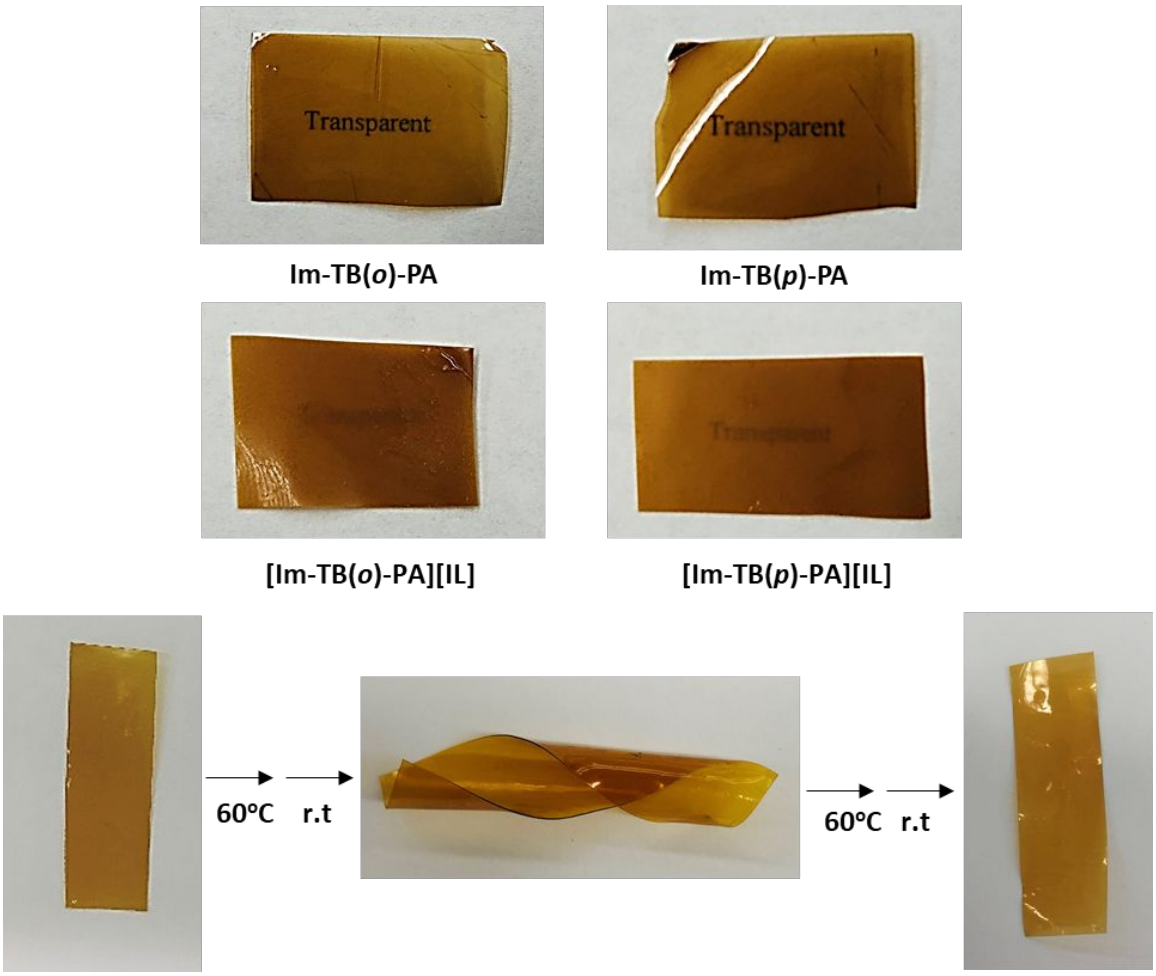

Figure 2. Photographs of newly developed Im-TB-PA ionenes and their "free" IL composite membranes together with the shape memory property.

3.3. Thermal and Physical Properties. The thermal stabilities of both the newly developed neat Im-TB-PA ionenes and corresponding composite membranes were investigated by thermogravimetric analysis (TGA) under a N_2 atmosphere, and the respective TGA profiles are depicted in Figure 3 according to the weight loss relative to temperature. All of the membranes demonstrated high thermal stabilities up to 330 ^{O}C with similar three-stage degradations irrespective of their macromolecular structure and molecular composition, except for [Im-TB(*p*)-PA]+[IL]. The first stage of weight loss was occurred between 330 - 430 ^{O}C corresponding to the decomposition of the TB groups from the major ionene backbone.[53] The second stage weight loss occurred between 430 ^{O}C and 490 ^{O}C and according to Cao et al. was primarily due to the

decomposition of the imidazolium cations and Tf_2N anions.[69] Finally, the third degradation at an elevated temperature 500 ^{O}C was attributed to the degradation of the residual amide segments and ionic chars.[53, 70] In contrast, a two-stage degradation profile was observed for [Im-TB(*p*)-PA]+[IL] membrane, in which free IL is blended with ionenes having Im-TB units at the *para* position, a similar trend was observed with our previously reported ionenes.[65] As shown in Figure 3, in this composition, both major ionene backbone and ionic moieties underwent a combined single degradation between 350 - 490 ^{O}C, followed by the degradation of the residual amide segments from 500 ^{O}C. This was attributed plausibly due to the increased ionic interactions and H-bonding, creating a characteristic organization of the polymer chains. Overall, the TGA results revealed that all the newly developed ionene membranes are adequately stable for permeation tests.

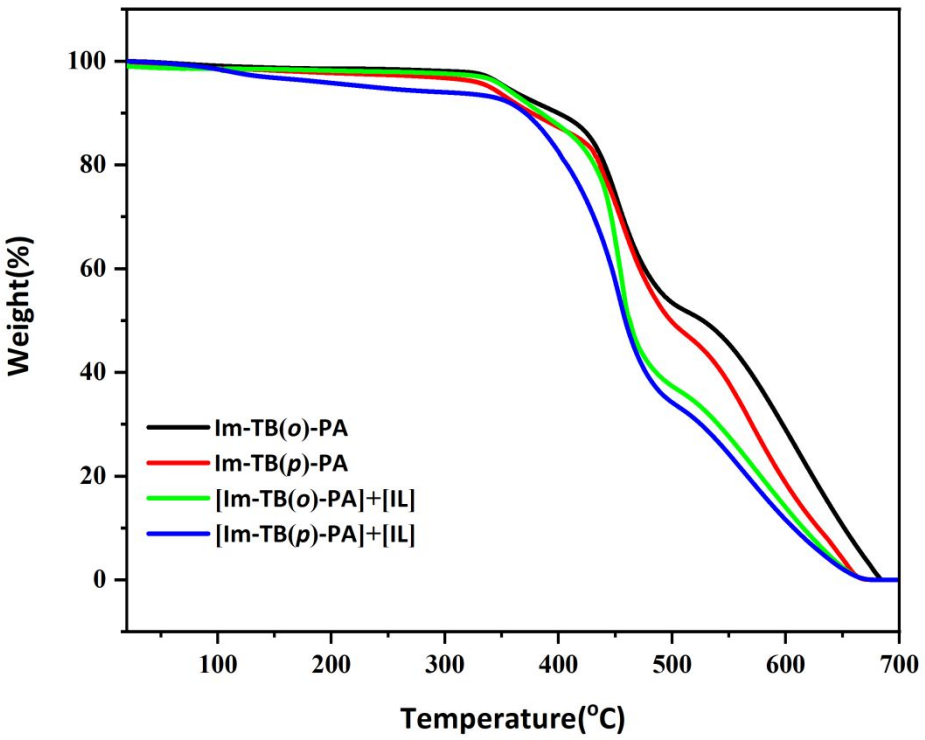

Figure 3. TGA profiles of the newly developed Im-TB-PA ionenes and their "free" IL composite membranes.

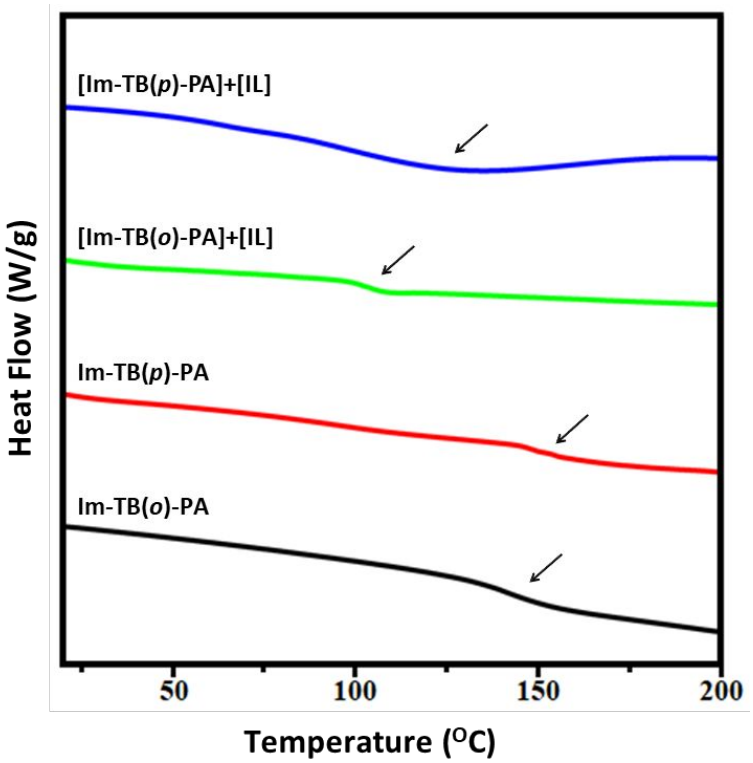

Figure 4. DSC curves of the newly developed Im-TB-Ionenes and their "free" IL composite membranes.

Further, the thermal transition properties of all the novel ionene membranes as a function of amide linkage as well as free IL incorporation in the ionene were analyzed by DSC measurements (Figure 4 and Table 1). It is well-known that the DSC measurements usually reflect the polymer chain mobility as well as phase behavior of polymer blends, and the quantified glass transition temperature (T_g) values are mainly resulted by the polymer chain rigidity and/or the interchain interactions. In this study, it was interesting to find high T_g values (~150 ^{o}C) for both the newly developed Im-TB-PA ionenes, much higher than those obtained from other Im-TB-ionenes (~100 ^{o}C), according to our previously reported work.[53] Although there were no much difference in T_g values observed with varying the regiochemistry of the ionenes either 'ortho' or 'para' derivative, this result clearly suggested that the integration of Im-TB-ionenes into intrinsic polymer chains such as amide-linkages drastically increased the thermal transition properties. Nonetheless, as

summarized in Table 1, both the composite membranes ([Im-TB(*o*&*p*)-PA]+[IL]) have reduced T_g values, indicating an enhancement in polymer chain mobility upon the incorporation of free ILs. Most importantly, [Im-TB(*o*&*p*)-PA]+[IL] membranes displayed a single T_g, proving that free ILs were well miscible in the newly developed Im-TB-PA ionene matrices, and no crystalline behavior was observed (Figure 4). Li et al. also reported a similar behavior that incorporation of free ILs (i.e., non-polymerizable ILs) in poly(IL)s instigate an improvised polymer chain flexibility and lower the T_g values because free ILs acted as nonvolatile selective plasticizing agents.[71] This tendency further related to gas transport properties of corresponding membranes; a drastic enhancement of permeability was obtained due to high diffusivity coefficients hailed from improved polymer chain flexibility. Our gas permeability test also confirms that free IL incorporation in Im-TB-PA ionenes corresponds to high gas permeability, as discussed in the following sections. At the same time, despite the plasticizing phenomenon with free IL blends, PA ionene having Im-TB units at the '*para*' position ([Im-TB(*p*)-PA]+[IL]) showed less reduction in T_g value (128.2, Table 1) due to enhanced ionic interactions and/or H-bonding, according to the DSC analysis.

Table 1. Physical property studies that quantified for the newly developed Im-TB-PA ionenes and corresponding composites.

Membranes	Weight Ratio (wt% ionene : wt% IL)	T_g (^{O}C)	d-spacing (Å)	Remaining Mass After Gas Separation Tests (%)
Im-TB(*o*)-PA Neat	100 : 0	148.8	5.94	99.3
Im-TB(*p*)-PA Neat	100 : 0	152.5	5.85	99.4
[Im-TB(*o*)-PA]+[IL]	60 : 40	102.4	6.05	99.1
[Im-TB(*p*)-PA]+[IL]	60 : 40	128.2	6.02, 4.75	99.1

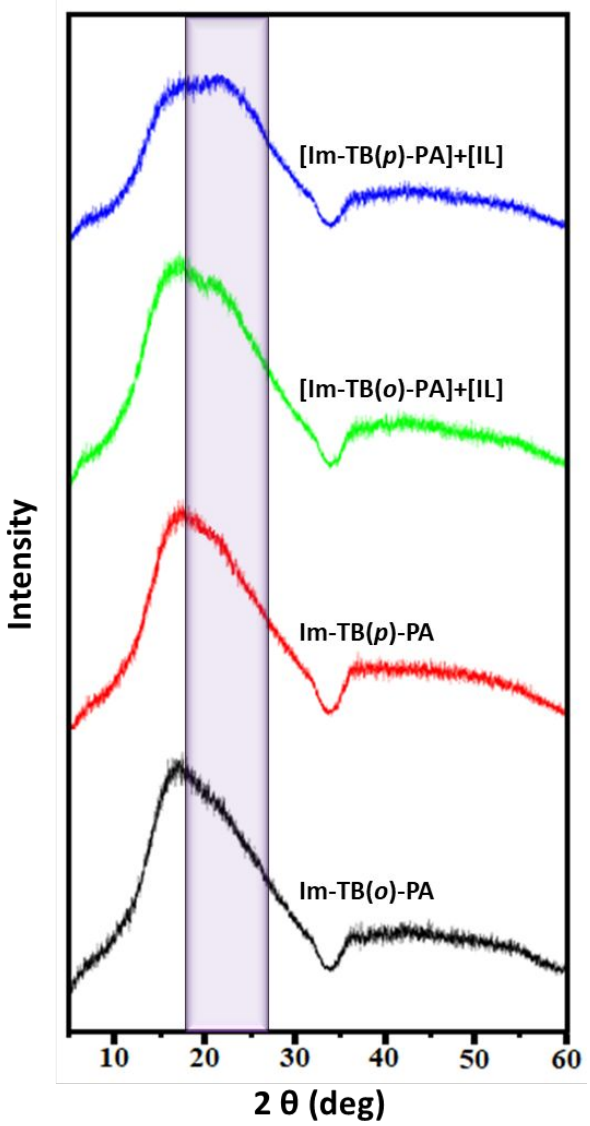

Figure 5. Wide-angle X-ray diffraction plots obtained from the newly developed Im-TB-PA ionenes and corresponding composites.

In order to quantify the changes in the polymer chain packing conditions, the newly developed Im-TB-PA ionenes and their IL composites were further examined by wide-angle X-ray diffraction (WAXD) analysis depicted in Figure 5. The absence of sharp diffraction peaks confirmed that both the neat Im-TB(*o*&*p*)-PA ionenes and their free IL composites [Im-TB(*o*&*p*)-PA]+[IL] were totally amorphous. While the neat Im-TB(*o*&*p*)-PA ionenes displayed a single-peak distribution, a bimodal distribution or an extra shoulder peak was obtained for IL composites [Im-TB(*o*&*p*)-

PA]+[IL], plausibly because of the formation of new clusters of micro-structure within the amorphous Im-TB-PA ionenes or altered polymer chain mobility of ionenes upon the incorporation of free ILs.[72] The intersegmental (d)-spacing values of [Im-TB(*o*&*p*)-PA]+[IL] membranes calculated from the main halo were found slightly higher values irrespective of their molecular ionene structure although an additional d-spacing value from extra shoulder peak was found for [Im-TB(*p*)-PA]+[IL] membrane (Table 1). This analysis was in a good agreement with the DSC data obtained for [Im-TB(*o*&*p*)-PA]+[IL] membranes. These results conclude that the incorporation of free ILs served to create and fill more volume within the ionene matrix, expecting an enhancement in their gas diffusivities and hence permeabilities. The detailed discussion of gas permeation behaviors of all the ionene membranes developed in this study is well described below. Later, the physical stability of these Im-TB-PA ionene membranes and their "free" IL counterparts was also quantified by measuring mass loss before and after the gas separation tests. The resulting high residual mass (>99%) of each membrane summarized in Table 1, an evidence of high mechanical stability of novel Im-TB-PA ionene and their IL composite membranes.

3.4. Gas Transport Properties and CO_2 Separation Performance of Im-TB-PA ionenes and their Free IL Composite Analogues. An ideal membrane in the gas separation process needs to exhibit a high permeability and a high selectivity simultaneously to facilitate a cost-effective separation process. In this study, the gas separation properties of newly developed Im-TB-PA ionenes and their free IL composites were quantified using a lab-made high-vacuum time-lag unit according to a constant volume/variable-pressure method. The pure gas permeabilities of CO_2 and other light gases including H_2, N_2, and CH_4, and permselectivities of CO_2/H_2, CO_2/N_2, and CO_2/CH_4 were measured and summarized in Table 2. To better understand the CO_2 separation

behaviors of these novel membranes, we also calculated the diffusivity coefficients using the time lag equation (eq. 2 in Experimental Section) and subsequently determined the solubility coefficients by assuming a solution-diffusion transportation model ($P = SD$), and reported in Table 3.

CO_2 is a polar gas with a quadrupole moment and exhibits higher condensability than other light gases (H_2, N_2, and CH_4) due to its critical properties (T_c = 31.1 ^oC, P_c = 72.9 atm). To prepare CO_2-selective separation membranes, rubbery polymers, or certain polar functional polymers such as poly(IL)s are widely been used in order to interact with the quadrupolar CO_2 molecules, and hence, boost the CO_2 solubilities.[73-75] The obtained results revealed that the CO_2 solubility in such polymers is even one to two orders of magnitude higher than that of the other light gases, which further enhances CO_2 permeability. On the other hand, it has been proven that the introduction of "free" ILs into neat poly(IL)s increases CO_2 permeability dramatically with little-to-no sacrifice in CO_2/light gas selectivity.[76] Many studies have evidenced this trend due to enhanced diffusivity coefficients caused by high free volume distribution and/or improved polymer chain mobility in polymer composite matrix.[76-79] Similarly, in the present work, the incorporation of free ILs into novel Im-TB-PA ionenes were anticipated to have an enhanced diffusivity together with high CO_2 solubility, which could be favorable for a reverse-selectivity behavior despite the kinetic diameter order of the respective gas molecules: H_2 (2.89 Å) > CO_2 (3.3 Å) > N_2 (3.6 Å) > CH_4 (3.8 Å).

Looking at the permeability results obtained for the Im-TB-PA ionenes and their IL composites, CO_2 displayed the highest gas permeability among the four gases, considerably higher than that of H_2 with a smaller diameter, suggesting the high CO_2-philic behaviors of the newly developed

ionenes and their free IL composite analogues (see Table 2). While the gas permeabilities of neat Im-TB-PA ionenes displayed a similar result irrespective of their *ortho* and *para* connectivity, their free IL composite analogues exhibited a dramatic increase in permeabilities. For example, the CO_2 permeabilities of Im-TB(*o*)-PA and Im-TB(*p*)-PA were 5.27 and 4.87 barrer, respectively. Whereas, [Im-TB(*o*)-PA]+[IL] and [Im-TB(*p*)-PA]+[IL] obtained much higher CO_2 permeabilities of 47.19 and 21.13 barrer, respectively. It is noteworthy that the permeabilities of all the gases to the [Im-TB(*o*)-PA]+[IL] composite membrane were found to have a drastic increase compared to its Im-TB(*o*)-PA counterpart (Table 2). This extraordinary trend corresponded to a significant increase in the diffusivity coefficients (see Table 3), plausibly caused by the irregularity in the interchain spacing and/or the polymer chain flexibility in the Im-TB(*o*)-PA ionene matrix upon the incorporation of free IL. Indeed, this result was consistent with the d-spacing data and the thermal transition properties of newly developed ionene systems (much lower T_g was obtained for [Im-TB(*o*)-PA]+[IL]).

At the same time, in contrast to the molecular-sieving mechanism, the permeability of each single gas for both the ionene- IL composite membranes found in the order of $P_{CO2} > P_{H2} >> P_{CH4} > P_{N2}$ (Table 2). The CH_4 permeability was slightly higher than that of N_2 although the permeability of composite membranes was primarily dependent on the gas dissolution into the dense membrane and the gas diffusion through it. In this case, the differences in permeability between CH_4 and N_2 gases mainly arose from the solubility differences of each gas species, a much higher solubility was obtained for CH_4 while yielding a similar diffusivity of N_2 (see Table 3). As a result, a reverse-selectivity favorable of CO_2/N_2 separation than CO_2/CH_4 was found for both the newly developed [Im-TB(*o&p*)-PA]+[IL] composite membranes. A similar trend of high CH_4 permeability and

hence favorable CO_2/N_2 separation performance was also reported for several other poly(IL)-IL composite membranes.[76, 77, 79]

Table 2. Pure gas permeabilities (P)[a] and permselectivities (α) of Im-TB-PA ionene polymer membranes at 3 atm and 20°C
[a] *P* in barrers, where 1 barrer = 10^{-10} [cm^3 (STP) cm]/(cm^2 s cm Hg)

Membrane	P_{CO2}	P_{H2}	P_{N2}	P_{CH4}	$\alpha_{CO2/H2}$	$\alpha_{CO2/N2}$	$\alpha_{CO2/CH4}$
Im-TB(*o*)-PA	5.27	1.99	0.116	0.093	2.65	45.43	56.67
Im-TB(*p*)-PA	4.87	1.808	0.097	0.079	2.69	50.08	61.62
[Im-TB(*o*)-PA]+[IL]	47.19	10.78	0.912	1.01	4.38	51.74	46.73
[Im-TB(*p*)-PA]+[IL]	21.13	5.43	0.372	0.485	3.89	56.84	43.57

Table 3. Pure gas diffusivity coefficients[a] and solubility coefficients[b] with their ideal selectivities at 3 atm and 20 °C

Membrane	D_{CO2}	D_{N2}	D_{CH4}	S_{CO2}	S_{N2}	S_{CH4}	$D_{CO2/N2}$	$D_{CO2/CH4}$	$S_{CO2/N2}$	$S_{CO2/CH4}$
Im-TB(*o*)-PA	1.12	0.221	0.191	4.71	0.525	0.487	5.07	5.86	8.97	9.67
Im-TB(*p*)-PA	0.981	0.201	0.183	4.96	0.483	0.432	4.88	5.36	10.27	11.48
[Im-TB(*o*)-PA]+[IL]	9.217	1.92	1.80	5.12	0.475	0.561	4.8	5.12	10.78	9.13
[Im-TB(*p*)-PA]+[IL]	3.92	0.838	0.802	5.39	0.444	0.605	4.89	4.95	12.14	8.91

[a]Diffusivity coefficient (10^{-8} cm^2/s). [b]Solubility coefficient (10^{-2} cm^3 (STP) cm^{-3} cm^{-1} Hg^{-1})

Nonetheless, as can be seen in Table 3, the newly developed Im-TB-PA ionenes and their IL composite membranes exhibited much higher CO_2 solubility than the N_2, or CH_4 solubilities, due to a stronger affinity of ionic liquid groups toward quadrupolar CO_2 molecules. In other words, a solubility-controlled mechanism was constructively contributed despite the molecular substructure and molecular composition of newly developed ionene systems. Subsequently, all the ionene membranes developed in this study displayed excellent CO_2 permselectivities over N_2 and CH_4

gases. Most importantly, an enhanced CO_2/N_2 selectivity was obtained for both [Im-TB(*o*&*p*)-PA]+[IL] composite membranes due to improved solubility selectivity (Table 3). It is also noteworthy that high CO_2 solubility of these ionenes favorably resulted in a reverse-selectivity toward CO_2/H_2 gas pair as well (Table 2).

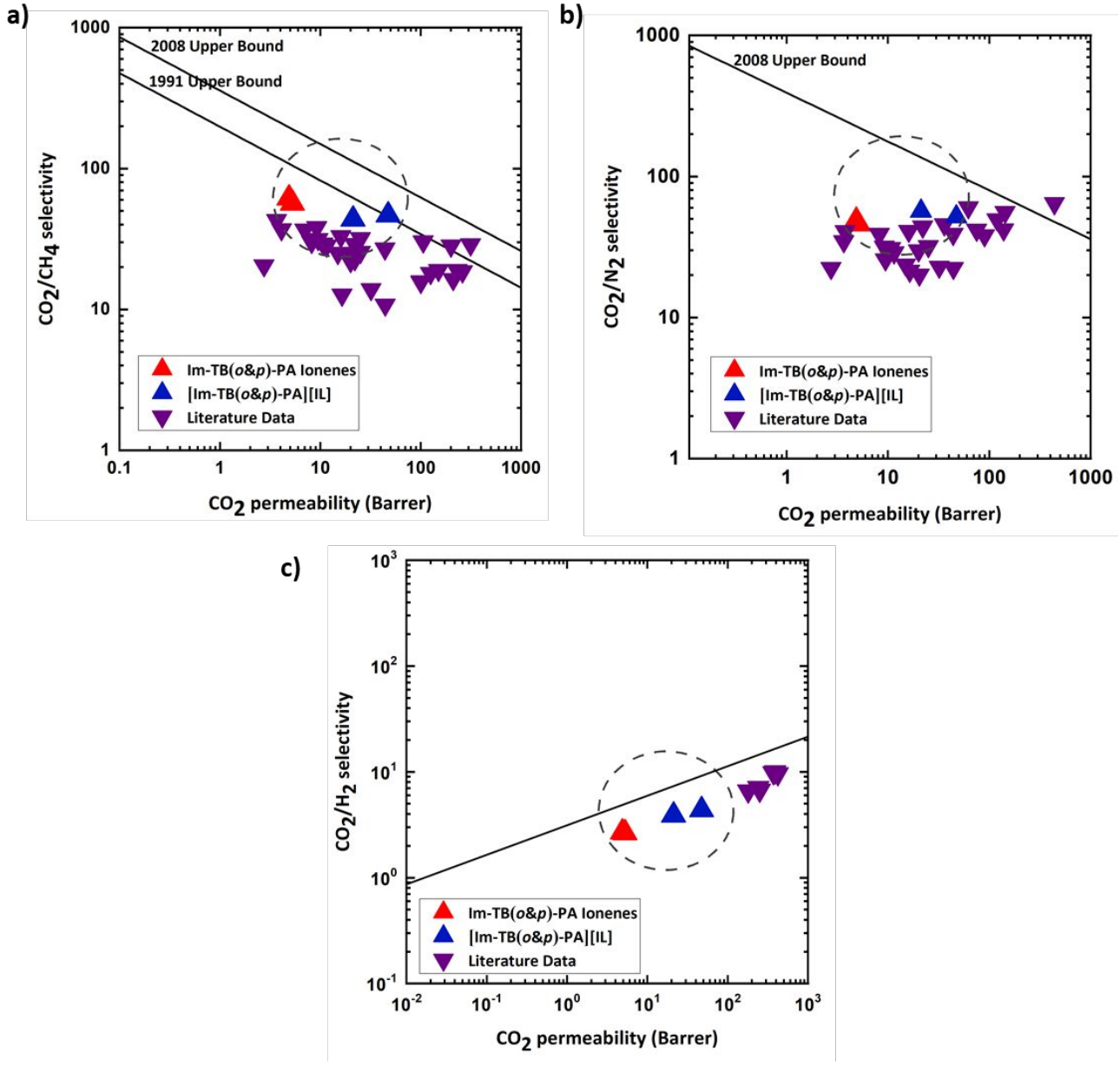

Figure 6. CO_2 separation performance of the newly developed Im-TB-PA ionenes and their free IL composites depicted on the CO_2/CH_4 (a), CO_2/N_2 (b), and CO_2/H_2 (c) "Upper Bound" plots. The key literature data reported for other ioinenes, poly(IL)s, and poly(IL)-IL membranes also were depicted.

As portrayed in Figure 6, the CO_2 permeability-selectivity tradeoff results obtained for CO_2/CH_4, CO_2/N_2, and CO_2/H_2 gas pairs were then compared by plotting the benchmark upper bound of the Robeson plot and the upper bound proposed by Freeman, et al.[14, 15, 80] The key literature reports related to other imidazolium-based ionenes,[81] poly(IL)s,[44, 62] and poly(IL)-IL composites[76-78] were also included for comparison. The trade-off plots demonstrated that the permeability-selectivity values of the Im-TB-PA ionenes and their IL composite membranes fell below the 2008 upper bound lines for CO_2/CH_4 and CO_2/N_2 gas pairs, however, their performance was comparable and within the general range of other poly(IL)s and the ionenes. At the same time, the [Im-TB(*o*)-PA]+[IL] membrane curve appeared above the 1991 upper bound for CO_2/CH_4 gas pair because of improved permeability (47.19 barrer) with the little-to-no sacrifice of selectivity (46.73) upon the incorporation of free IL (Figure 6(a)). Besides, the CO_2 separation performance of these novel materials reached the reverse CO_2/H_2 upper bound limit (Figure 6(c)). Overall, the gas permeation results revealed that the newly developed ionene membranes, particularly, free IL composite of *ortho*-connected Im-TB-PA ionene have remarkable capacity toward selective CO_2 separation in practical applications such as natural gas/biogas (i.e., CO_2/CH_4), flue gas (i.e., CO_2/N_2), and syngas (i.e., CO_2/H_2) streams.

4. CONCLUSIONS

In conclusion, a facile synthetic procedure to prepare two novel imidazolium-mediated Tröger's base-based ionenes having aromatic amide linkages was employed, yielding polymers with high molecular weight and excellent solubility in many polar organic solvents. These materials were successfully demonstrated for their potential utility to separate CO_2 gas molecules in the form of "neat" ionene as well as "free" IL composite membranes. We investigated the effects of Im-TB-

PA ionenes and their IL composite counterparts on the structures and properties of the polymers as well as the gas separation behaviors with varying the regiochemistry of imidazolium groups in TB units at either *ortho* or *para* positions. The results showed that Im-TB-PA ionenes were compatible with free ILs, producing homogeneous and mechanically stable blend membranes with improved CO_2 permeabilities without any impairments in permselectivities. Indeed, an enhancement in CO_2/N_2 selectivity was obtained for both [Im-TB(*o*&*p*)-PA]+[IL] composite membranes due to increased solubility selectivity. Considering the good CO_2/CH_4, CO_2/N_2, and CO_2/H_2 permselectivites obtained and the facile polymer synthesis with subsequent membrane procedure, this simple strategy can be readily applied toward preparing more extraordinary ionene-based membranes for CO_2 separation applications.

Lastly, taking into the account of the versatility and functionality of the membranes prepared from the newly developed Im-TB-PA ionenes with excellent thermal and mechanical stabilities, paving new possibilities to the developments of novel materials with a wide range of applications. Most notably, the shape memory in certain temperature ranges of Im-TB(*o*)-PA ionene is furthered with the application of heat. As these fascinating physical features were recognized, our research findings on Im-TB-PA ionenes foresee to the countless applications beyond gas separation such as coatings,[82, 83] impact-resistant materials,[84] 3D-printing feeds[85] or catalysis.[57]

CONFLICTS OF INTEREST

There are no conflicts to declare.

ACKNOWLEDGMENTS

This material is based upon work supported by the U.S. Department of Energy, Office of Science, Office of Basic Energy Sciences, Separation Science program under Award Number DE-SC0018181. Additional support from NASA Marshall Space Flight Center (CAN 80MSFC18M0041) for thermal analysis, and the National Science Foundation from the Major Research Instrumentation Program (CHE-1726812) for purchase of the MALDI/TOF-TOF mass spectrometer is gratefully acknowledged.

NOTES AND REFERENCES

1. E. D. Bates, R. D. Mayton, I. Ntai and J. H. Davis, *J. Am. Chem. Soc.*, 2002, **124**, 926-927.
2. S. Ma'mun, V. Y. Dindore and H. F. Svendsen, *Ind. Eng. Chem. Res.*, 2007, **46**, 385-394.
3. T. E. Rufford, S. Smart, G. C. Y. Watson, B. F. Graham, J. Boxall, J. C. Diniz da Costa and E. F. May, *J. Petrol. Sci. Eng.*, 2012, **94-95**, 123-154.
4. R. Khalilpour, K. Mumford, H. Zhai, A. Abbas, G. Stevens and E. S. Rubin, *J. Clean. Prod.*, 2015, **103**, 286-300.
5. D. Aaron and C. Tsouris, *Sep. Sci. Technol.*, 2005, **40**, 321-348.
6. Y. Zhang, J. Sunarso, S. Liu and R. Wang, *Int. J. Greenh. Gas Control.*, 2013, **12**, 84-107.
7. Q. Sun, H. Li, J. Yan, L. Liu, Z. Yu and X. Yu, *Renew. Sust. Energ. Rev.*, 2015, **51**, 521-532.
8. H. Yang, Z. Xu, M. Fan, R. Gupta, R. B. Slimane, A. E. Bland and I. Wright, *J. Environ. Sci.*, 2008, **20**, 14-27.
9. A. Singh and K. Stéphenne, *Energy Procedia*, 2014, **63**, 1678-1685.
10. M. Campbell, *Energy Procedia*, 2014, **63**, 801-807.
11. L. Riboldi and O. Bolland, *Int. J. Greenh. Gas Control.*, 2015, **39**, 1-16.

12. M. Tagliabue, D. Farrusseng, S. Valencia, S. Aguado, U. Ravon, C. Rizzo, A. Corma and C. Mirodatos, *Chem. Eng. J.*, 2009, **155**, 553-566.

13. A. Hart and N. Gnanendran, *Energy Procedia*, 2009, **1**, 697-706.

14. L. M. Robeson, *J. Membr. Sci.*, 1991, **62**, 165-185.

15. L. M. Robeson, *J. Membr. Sci.*, 2008, **320**, 390-400.

16. S. Sridhar, T. M. Aminabhavi and M. Ramakrishna, *J. Appl. Polym.*, 2007, **105**, 1749-1756.

17. M. Iqbal, Z. Man, H. Mukhtar and B. K. Dutta, *J. Membr. Sci.*, 2008, **318**, 167-175.

18. S. Sridhar, B. Smitha, M. Ramakrishna and T. M. Aminabhavi, *J. Membr. Sci.*, 2006, **280**, 202-209.

19. T. Nakagawa, T. Saito, S. Asakawa and Y. J. Saitom, Gas Separ. Purif. 1988, **2**, 3-8.

20. Y. Gupta, R. Wakeman and K. Hellgardt, *Desalination*, 2006, **199**, 474-476.

21. C. M. Zimmerman and W. J. Koros, *J. Polym. Sci. Poly. Phys.*, 1999, **37**, 1235-1249.

22. H. Lin and B. D. Freeman, *J. Membr. Sci.*, 2004, **239**, 105-117.

23. Z. Y. Wang, P. R. Moulinie and Y. P. Handa, *J. Polym. Sci. Poly. Phys.*,1998, **36**, 425-431.

24. C. Camacho-Zuñiga, F. A. Ruiz-Treviño, S. Hernández-López, M. G. Zolotukhin, F. H. J. Maurer and A. González-Montiel, *J. Membr. Sci.*, 2009, **340**, 221-226.

25. J. Espeso, A. E. Lozano, J. G. de la Campa and J. de Abajo, *J. Membr. Sci.*, 2006, **280**, 659-665.

26. D. Bera, V. Padmanabhan and S. Banerjee, *Macromolecules*, 2015, **48**, 4541-4554.

27. R. Wang, C. Cao and T.-S. Chung, *J. Membr. Sci.,* 2002, **198**, 259-271.

28. Y. Zhuang, J. G. Seong and Y. M. Lee, *Prog. Polym. Sci.*, 2019, **92**, 35-88.

29. N. B. McKeown and P. M. Budd, *Chem. Soc. Rev.*, 2006, **35**, 675-683.

30. P. Budd, K. Msayib, C. Tattershall, B. Ghanem, K. Reynolds, N. McKeown and D. Fritsch, *J. Membr. Sci.*, 2005, **251**, 263-269.

31. N. Du, G. P. Robertson, J. Song, I. Pinnau and M. D. Guiver, *Macromolecules*, 2009, **42**, 6038-6043.

32. N. B. McKeown and P. M. Budd, *Macromolecules*, 2010, **43**, 5163-5176.

33. B. S. Ghanem, N. B. McKeown, P. M. Budd, J. D. Selbie and D. Fritsch, *Adv. Mater.*, 2008, **20**, 2766-2771.

34. C. G. Bezzu, M. Carta, A. Tonkins, J. C. Jansen, P. Bernardo, F. Bazzarelli and N. B. McKeown, *Adv. Mater.*, 2012, **24**, 5930-5933.

35. M. Carta, R. Malpass-Evans, M. Croad, Y. Rogan, J. C. Jansen, P. Bernardo, F. Bazzarelli and N. B. McKeown, *Science*, 2013, **339**, 303-307.

36. Y. Zhuang, J. G. Seong, Y. S. Do, H. J. Jo, Z. Cui, J. Lee, Y. M. Lee and M. D. Guiver, *Macromolecules*, 2014, **47**, 3254-3262.

37. R. Williams, L. A. Burt, E. Esposito, J. C. Jansen, E. Tocci, C. Rizzuto, M. Lanč, M. Carta and N. B. McKeown, *J. Mater. Chem. A*, 2018, **6**, 5661-5667.

38. Z. Wang, D. Wang and J. Jin, *Macromolecules*, 2014, **47**, 7477-7483.

39. Z. Wang, D. Wang, F. Zhang and J. Jin, *ACS Macro Lett.*, 2014, **3**, 597-601.

40. X. Ma, M. Abdulhamid, X. Miao and I. Pinnau, *Macromolecules*, 2017, **50**, 9569-9576.

41. J. E. Bara, T. K. Carlisle, C. J. Gabriel, D. Camper, A. Finotello, D. L. Gin and R. D. Noble, *Ind. Eng. Chem. Res.*, 2009, **48**, 2739-2751.

42. P. Scovazzo, *J. Membr. Sci.*, 2009, **343**, 199-211.

43. P. Cserjési, N. Nemestóthy and K. Bélafi-Bakó, *J. Membr. Sci.*, 2010, **349**, 6-11.

44. J. E. Bara, C. J. Gabriel, E. S. Hatakeyama, T. K. Carlisle, S. Lessmann, R. D. Noble and D. L. Gin, *J. Membr. Sci.*, 2008, **321**, 3-7.

45. P. Li and M. R. Coleman, *Eur. Polym. J.*, 2013, **49**, 482-491.

46. I. Kammakakam, H. W. Kim, S. Nam, H. B. Park and T.-H. Kim, *Polymer*, 2013, **54**, 3534-3541.

47. L. Liang, Q. Gan and P. Nancarrow, *J. Membr. Sci.*, 2014, **450**, 407-417.

48. I. Kammakakam, S. Nam and T.-H. Kim, *RSC Adv.*, 2015, **5**, 69907-69914.

49. M. S. Mittenthal, B. S. Flowers, J. E. Bara, J. W. Whitley, S. K. Spear, J. D. Roveda, D. A. Wallace, M. S. Shannon, R. Holler, R. Martens and D. T. Daly, *Ind. Eng. Chem. Res.*, 2017, **56**, 5055-5069.

50. K. E. O'Harra, I. Kammakakam, E. M. Devriese, D. M. Noll, J. E. Bara and E. M. Jackson, *Membranes (Basel)*, 2019, **9**.

51. I. Kammakakam, K. E. O'Harra, G. P. Dennis, E. M. Jackson and J. E. Bara, *Polym. Int.*, 2019, **68**, 1123-1129.

52. K. E. O'Harra, I. Kammakakam, D. M. Noll, E. M. Turflinger, G. P. Dennis, E. M. Jackson and J. E. Bara, *Membranes (Basel)*, 2020, **10**.

53. I. Kammakakam, K. E. O'Harra, J. E. Bara and E. M. Jackson, *ACS Omega*, 2019, **4**, 3439-3448.

54. M. Carta, M. Croad, J. C. Jansen, P. Bernardo, G. Clarizia and N. B. McKeown, *Polym. Chem.*, 2014, **5**.

55. X. Zhu, C.-L. Do-Thanh, C. R. Murdock, K. M. Nelson, C. Tian, S. Brown, S. M. Mahurin, D. M. Jenkins, J. Hu, B. Zhao, H. Liu and S. Dai, *ACS Macro Lett.*, 2013, **2**, 660-663.

56. A. Del Regno, A. Gonciaruk, L. Leay, M. Carta, M. Croad, R. Malpass-Evans, N. B. McKeown and F. R. Siperstein, *Ind. Eng. Chem. Res.*, 2013, **52**, 16939-16950.

57. M. Carta, M. Croad, K. Bugler, K. J. Msayib and N. B. McKeown, *Polym. Chem.*, 2014, **5**.

58. F. Xia, M. Pan, S. Mu, R. Malpass-Evans, M. Carta, N. B. McKeown, G. A. Attard, A. Brew, D. J. Morgan and F. Marken, *Electrochim. Acta*, 2014, **128**, 3-9.

59. Y. Rong, R. Malpass-Evans, M. Carta, N. B. McKeown, G. A. Attard and F. Marken, *Electroanalysis*, 2014, **26**, 904-909.

60. M. R. Esfahani, A. Taylor, N. Serwinowski, Z. J. Parkerson, M. P. Confer, I. Kammakakam, J. E. Bara, A. R. Esfahani, S. N. Mahmoodi, N. Koutahzadeh and M. Z. Hu, *ACS Sustain. Chem. Eng.*, 2020, **8**, 4225-4235.

61. Y. Misawa, N. Koumura, H. Matsumoto, N. Tamaoki and M. Yoshida, *Macromolecules*, 2008, **41**, 8841-8846.

62. J. E. Bara, S. Lessmann, C. J. Gabriel, E. S. Hatakeyama, R. D. Noble and D. L. Gin, *Ind. Eng. Chem. Res.*, 2007, **46**, 5397-5404.

63. S. Zhao, J. Liao, D. Li, X. Wang and N. Li, *J. Membr. Sci.*, 2018, **566**, 77-86.

64. I. Kammakakam, A. H. N. Rao, H. W. Yoon, S. Nam, H. B. Park and T.-H. Kim, *Macromol. Res.*, 2014, **22**, 907-916.

65. K. E. O'Harra, I. Kammakakam, J. E. Bara and E. M. Jackson, *Polym. Int.*, 2019, **68**, 1547-1556.

66. Y. Shibasaki, T. Mori, A. Fujimori, M. Jikei, H. Sawada and Y. Oishi, *Macromolecules*, 2018, **51**, 9430-9441.

67. C. E. Zawaski, E. M. Wilts, C. A. Chatham, A. T. Stevenson, A. M. Pekkanen, C. Li, Z. Tian, A. R. Whittington, T. E. Long and C. B. Williams, *Polymer*, 2019, **176**, 283-292.

68. J. Herzberger, J. M. Sirrine, C. B. Williams and T. E. Long, *Progress in Polymer Science*, 2019, **97.**

69. Y. Cao and T. Mu, *Ind. Eng. Chem. Res.*, 2014, **53**, 8651-8664.

70. C.-W. Chang, G.-S. Liou and S.-H. Hsiao, *J. Mater. Chem.*, 2007, **17**, 1007-1015.

71. P. Li, K. P. Pramoda and T.-S. Chung, *Ind. Eng. Chem. Res.*, 2011, **50**, 9344-9353.

72. V. Garaev, S. Pavlovica, I. Reinholds and G. Vaivars, *IOP Conference Series: Materials Science and Engineering*, 2013, **49.**

73. T. T. Moore and W. J. Koros, *J. Appl. Polym. Sci.*, 2007, **104**, 4053-4059.

74. J. L. Anthony, E. J. Maginn and J. F. Brennecke, *J. Phys. Chem. B*, 2002, **106**, 7315-7320.

75. I. Kammakakam, S. Nam and T.-H. Kim, *RSC Adv.*, 2016, **6**, 31083-31091.

76. J. E. Bara, E. S. Hatakeyama, D. L. Gin and R. D. Noble, *Polym. Advan. Technol.*, 2008, **19**, 1415-1420.

77. L. C. Tomé, M. A. Aboudzadeh, L. P. N. Rebelo, C. S. R. Freire, D. Mecerreyes and I. M. Marrucho, *J. Mater. Chem. A*, 2013, **1**.

78. L. C. Tomé, M. Isik, C. S. R. Freire, D. Mecerreyes and I. M. Marrucho, *J. Membr. Sci.*, 2015, **483**, 155-165.

79. L. C. Tomé, D. Mecerreyes, C. S. R. Freire, L. P. N. Rebelo and I. M. Marrucho, *J. Membr. Sci.*, 2013, **428**, 260-266.

80. H. Lin, E. Van Wagner, B. D. Freeman, L. G. Toy and R. P. Gupta, *Science*, 2006, **311**, 639-642.

81. T. K. Carlisle, J. E. Bara, A. L. Lafrate, D. L. Gin and R. D. Noble, *J. Membr. Sci.*, 2010, **359**, 37-43.

82. P. C Varelidis, R. L. McCullough and C. D. Papaspyrides, *Compos. Sci. Technol.*, 1999, **59**, 1813-1823.

83. H. Zhang, J. Wang, X. Liu, Z. Wang and S. Wang, *Ind. Eng. Chem. Res.*, 2013, **52**, 10172-10180.

84. K. Soygun, G. Bolayir and A. Boztug, *J. Adv. Prosthodont*, 2013, **5**, 153-160.

85. P. Cruz, E. D. Shoemake, P. Adam and J. Leachman, *IOP conf. ser., Mater. sci. eng.*, 2015, **102**, 012020.

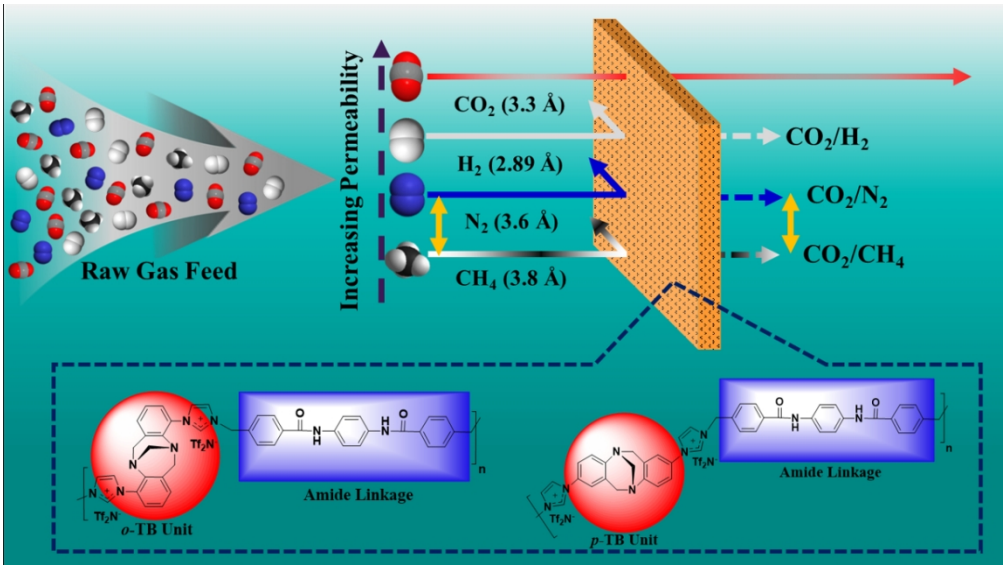
Raw Gas Feed
Increasing Permeability
CO2 (3.3 Å)
H2 (2.89 Å)
N2 (3.6 Å)
CH4 (3.8 Å)
CO2/H2
CO2/N2
CO2/CH4
Amide Linkage
o-TB Unit
p-TB Unit
Amide Linkage